

Tailoring Magnesium Nanoparticles In-Flight via Nonthermal Plasma for Enhanced Ignition

B. Wagner¹, P. Ghildiyal², M. Chowdhury², M. Kim³, M. Zachariah² and Lorenzo Mangolini^{1,3}

¹ Materials Science and Engineering Program, University of California Riverside, Riverside CA USA

² Department of Chemical and Environmental Engineering, University of California Riverside, Riverside CA USA

³ Department of Mechanical Engineering, University of California Riverside, Riverside CA USA

Abstract: Magnesium is a desirable fuel for energetics because of its high reactivity and high energy density, but its native oxide layer serves as a barrier for ignition. Our work involves the in-flight modification of magnesium nanoparticles by a nonthermal plasma process to circumvent the oxide layer formation and boost ignition performance. Core-shell magnesium-silicon oxide and hydrogenated magnesium nanoparticles were synthesized by a silane plasma and hydrogen plasma, respectively. Our findings show that the combustion properties and reaction kinetics can be tuned according to surface chemistry.

Keywords: Magnesium, coating, silicon oxide, magnesium hydride, energetics, ignition

1. Introduction

Improving nanoenergetics involving metal fuels focuses on managing the oxide layer because of its hinderance on combustion kinetics.[1] Magnesium (Mg) solid fuel has a lower boiling point temperature than its oxide, which forces it to leave by diffusion through its oxide shell during ignition.[2] This means that the rate-limiting step for Mg ignition is the Mg vapor transport through its oxide shell.[3] In order to achieve the full potential of Mg fuels, it is important to modify the surface to reduce the role of the oxide layer or eliminate it entirely. Applying coatings to Mg nanoparticles (NPs) could help alleviate the problem relating to the oxide shell, but there is little work in this area of research. Previous work by Hastings et al. involved coating Mg with siloxane by a vapor-solid interface reaction using cyclic hydridomethylsiloxanes as the precursor.[4] It was shown that the coatings improve stability, and there is no negative impact on the ignition temperature, though the reaction kinetics are accelerated.

Reducing particle size is another way of decreasing the diffusion lengths of atoms and accelerating reaction kinetics, though not without drawbacks. Particle agglomeration and sintering are issues that metal nanoparticles face for energetic applications, causing incomplete combustion of the active metal fuel.[5] One way of combating these problems is by using a gas generator, so that the rapid gas expansion during combustion helps reduce the agglomeration rate of fuel particles. This approach is explored by Young et al., in which nanoaluminum/nitrocellulose mesoparticles are synthesized by an electrospray method.[6] An energetic binder was used that generated gas during ignition, which promoted particle disintegration and reduced sintering of

the nanoparticles. Another pathway to generating gas during combustion of metal fuels is by incorporating hydrogen. Amorphous and crystalline silicon (Si) NPs were produced via silane nonthermal plasma by Xu et al.[7] Combustion of the Si NPs showed that the amorphous samples exhibited a higher rate of pressure generation. The large increase in peak pressure and pressurization rate is related to the amount of hydrogen content in the Si NPs. Amorphous Si NPs contain more SiH₂ and SiH₃, thus more hydrogen gas (H₂) is generated during combustion, resulting in increased pressure output.

Our work involves the in-flight functionalization of Mg NPs using nonthermal plasmas to address the aforementioned concerns regarding metal-based nanoenergetics. We constructed a thermal evaporation system equipped with a nonthermal plasma reactor to modify Mg in an oxygen-free environment. A silane plasma was utilized to coat Mg with a Si-based coating, which is allowed to oxidize upon air exposure. This Si-SiO_x coating not only limits the growth of a magnesium oxide (MgO) layer, but creates surface nanothermites. The direct contact between the Mg core fuel and Si-based oxidizer shell results in the drastic reduction in ignition temperature and hastened combustion kinetics with a primary oxidizer. Hydrogenated Mg NPs are also synthesized by employing a hydrogen plasma. These particles release H₂ during ignition, which results in higher pressurization rates versus pure Mg NPs. The in-flight surface modification of Mg enables us to tune the chemistry involved during ignition by tailoring the surface. This work highlights the untapped potential of non-thermal plasma processing for energetic applications.

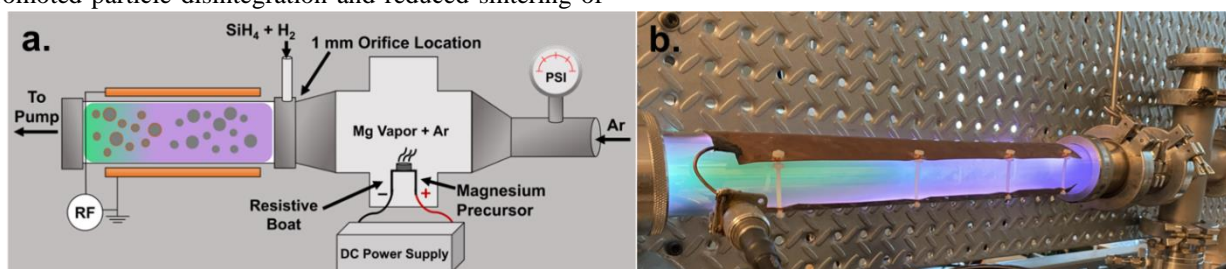


Figure 1. (a) Schematic of the thermal evaporator and plasma reactor system. (b) Photograph of the system in operation.

2. Experimental Details

Core-shell Mg nanoparticles were synthesized by gas-condensation of Mg vapor followed by a silane plasma for coating with Si. A schematic of the system is outlined in Figure 1a. Mg precursor was thermally evaporated by ohmic heating using a tungsten heating source, to which 74 A of DC current was applied. Subsequently, the Mg vapor was quenched using argon gas to homogeneously nucleate Mg nanoparticles. The Mg-laden aerosol was carried by argon gas through an orifice of 1 mm diameter for injection into the plasma reactor while flowing silane (1.36% in argon) and hydrogen gas. The plasma reactor was composed of 20" length quartz tubing with a 2" diameter. Radiofrequency (RF) at 60 W was supplied to copper parallel plate electrodes to produce plasma discharge. The pressure in the plasma reactor was ~1 Torr while the pressure in the evaporation chamber was ~40 Torr. The flow rates of the argon, silane, and hydrogen gases were 350 sccm, 60 sccm, and 30 sccm, respectively. Coated particles were collected onto a stainless-steel mesh filter and extracted after slowly leaking air to prevent ignition. The surface Si was then allowed to oxidize to produce a SiO_x-based shell.

For hydrogenated Mg NPs, the plasma system was altered to a 12" reactor tube and a copper ring electrode. The flow rate of Ar was 350 sccm and the H₂ flow rate was varied from 15-60 sccm. The pressure inside the evaporator chamber was ~40 Torr while the pressure in the plasma reactor was varied from 1-7 Torr. RF powers of 20-140 W were utilized to promote hydrogenation.

Ignition characterization of the in-flight modified Mg (Mg/Si-SiO_x) NPs was performed using the following instrumentation: temperature-jump time-of-flight mass spectrometry (T-jump TOFMS) to probe ignition mechanisms with a fast heating rate ($\sim 10^5$ °C s⁻¹), differential scanning calorimetry (DSC) to monitor the oxidation of the NPs under slow heating (10 °C min⁻¹), and a high-speed camera to view the ignition events. The combustion of Mg/Si-SiO_x NPs was tested against control samples of Mg and Si NPs, using bismuth oxide (Bi₂O₃) as the oxidizer. The combustion of hydrogenated Mg NPs was tested against Mg control samples in pressure-cell tests using copper oxide (CuO) as the oxidizer.

3. Results

3.1. Core-shell Mg Particles

Scanning transmission electron microscopy (STEM) equipped with an energy dispersive x-ray spectroscopy (EDS) detector were used to evaluate the coating of the Mg/Si-SiO_x NPs. Figure 2a shows STEM/EDS of the Mg control sample, which indicates there are Mg cores enveloped by magnesium oxide (MgO) shells. Figure 2b shows the Mg/Si-SiO_x NPs have magnesium cores surrounded by conformal Si-based shells. According to compositional analysis, the composition of the NPs is 10.5 % Si by mass. Typical thickness of the coating is 15-20 nm. The presence of a conformal coating demonstrates the

capability of nonthermal plasmas for in-flight modification of nanoparticles.

Ignition species were characterized using a T-jump TOFMS instrument in a time-resolved manner. Figure 3a and 3b show the Mg release and Bi release profiles for Mg/Si-SiO_x particles as well as the Mg and Si control samples during combustion with bismuth oxide (oxidizer). The results show that Mg and Bi release earlier for Mg/Si-SiO_x NPs than for the Mg control. The Si control released no Mg and minimal Bi during heating. The earlier onset of Mg release for the coated particles can be attributed to the magnesiothermic reduction of silica, which provides energy required to initiate release of Mg vapor from the core. The Mg control has a delayed release because Mg needs to vaporize within the core and pass through its oxide layer, which serves as a diffusion barrier to atoms. The rate-limiting step is diffusion across the MgO layer. However, this step is bypassed by application of the Si-based coating in anaerobic conditions, resulting in faster Mg vapor release and subsequent Bi release.

High-speed camera capture was utilized to view the temporal ignition events via optical emission. Figures 3d and 3e show images of the ignition of Mg NPs and Mg/Si-SiO_x NPs, respectively. The ignition temperatures were noted from the time optical emission began. The results indicate that the Mg particles ignited at ~740 °C, while coated Mg particles ignited at ~520 °C. Additionally, the ignition of Mg/Si-SiO_x NPs completed ~200 μs earlier than the Mg control.

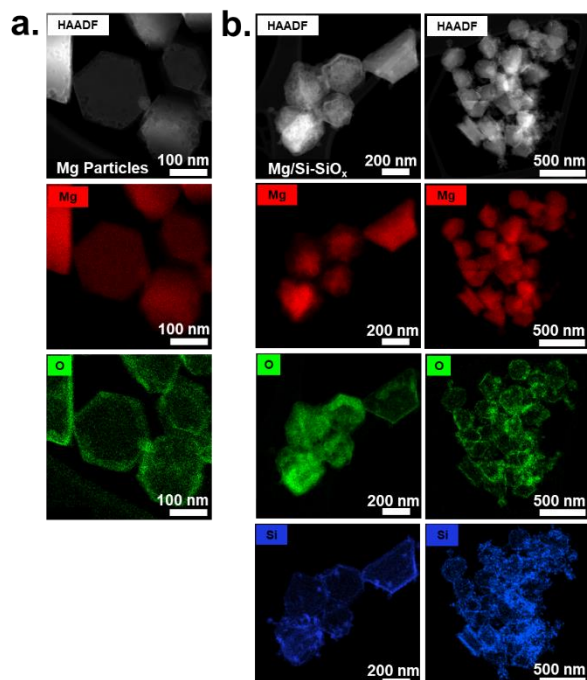


Figure 2. STEM/EDS pictographs showing (a) Mg NPs with a native oxide layer and (b) coated Mg NPs with a Si-based shell.

DSC compared the oxidation of Mg/Si-SiO_x NPs and a physical mixture containing Si NPs and Mg NPs. Figure 3c shows the DSC curves of the samples, in which there are two exothermic peaks for the Mg/Si-SiO_x NPs. The first peak occurs before the oxidation of the physical mixture sample, which is attributed to the intermetallic reaction between Mg core and surface Si. Afterward, the magnesiothermic reduction of silica is observed according to the large second exotherm. The results show that the oxidation of the Si-coated Mg is faster compared to the physical mixture. This suggests that the close proximity of the Si at the surface of the Mg particles allows for faster reaction kinetics.

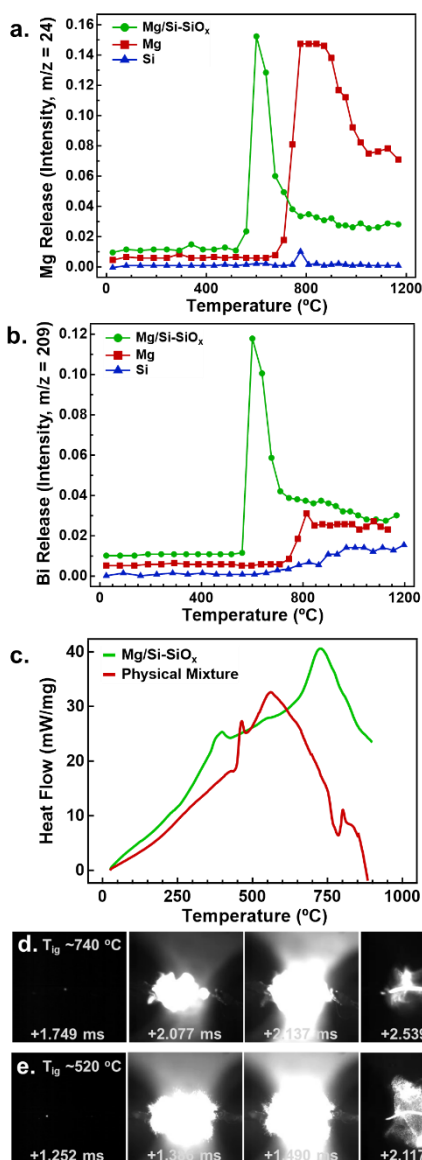


Figure 3. (a) Temporal Mg release and (b) Bi release of the coated Mg particles, Mg control, and Si controls samples from Tjump-TOFMS. (c) DSC of Mg/Si-SiO_x NPs and a physical mixture of Si NPs and Mg NPs. Images of the ignition events of (d) uncoated Mg NPs and (e) coated Mg NPs with Bi₂O₃.

3.2. Hydrogenated Mg Particles

Incorporation of magnesium hydride (MgH₂) into Mg particles was achieved by subjecting Mg-laden aerosols to a hydrogen discharge. Figure 4a shows x-ray diffraction (XRD) of Mg/MgH₂ NPs produced at varied RF power. The results indicate that increasing RF power produces more MgH₂. The peak area ratios of MgH₂:Mg are calculated and plotted in Figure 4b. Indeed, the content of MgH₂ in the Mg NPs increases with increasing RF, but the amount saturates at high power (above 80 W). Optical emission spectroscopy (OES) was used to monitor the atomic species within the plasma with respect to RF power. The intensity of the Mg and hydrogen (H) emission lines increased with increasing RF power. The peak ratio of the emission of Mg at 571 nm and the argon (Ar) emission at 763 nm was calculated. The observed trend showed the Mg:Ar increased with increasing RF power. Additionally, the peak ratio of the H emission at 656 nm and Ar emission at 763 nm was calculated, resulting in increasing H:Ar with increasing RF power (Figure 4c).

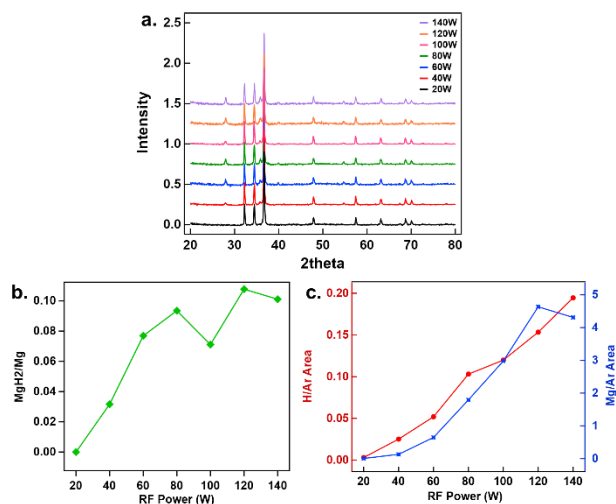


Figure 4. (a) XRD of hydrogenated Mg NPs synthesized using RF powers of 20-140 W. (b) Peak area ratios of the MgH₂:Mg from the XRD patterns of the different plasma power conditions. (c) The peak area ratios of H:Ar and Mg:Ar from OES emission lines.

Hydrogenated samples were subjected to ignition tests to evaluate their properties in comparison to a Mg control. Tjump-TOFMS was performed to monitor the ignition species, which showed Mg and H₂ release for the hydrogenated sample. The results show that H₂ releases at ~400 °C before the Mg at ~600 °C. This is expected because the desorption temperature of H₂ from MgH₂ is around 400 °C, which means the desorption of H₂ is important during the combustion of MgH₂-rich Mg NPs.[8] It is expected that the pressure generation during the combustion of Mg particles enriched with H₂ would be higher than pure Mg particles. Pressure cell tests were performed to analyze the peak pressure, pressurization rate, and burn time of the particles. As shown in Figure 5a, the peak pressure of hydrogenated Mg is slightly higher than

the Mg control, and the burn time was minimally shorter (Figure 5b). However, the pressurization rate was drastically increased (Figure 5c). The minimal increase in peak pressure is unsurprising because there is little MgH_2 within the sample. Despite this, the pressure is generated faster because of the H_2 release during ignition. Faster pressure generation is important for producing gas sooner during ignition to push nanoparticles outward, preventing it from agglomerating and sintering.

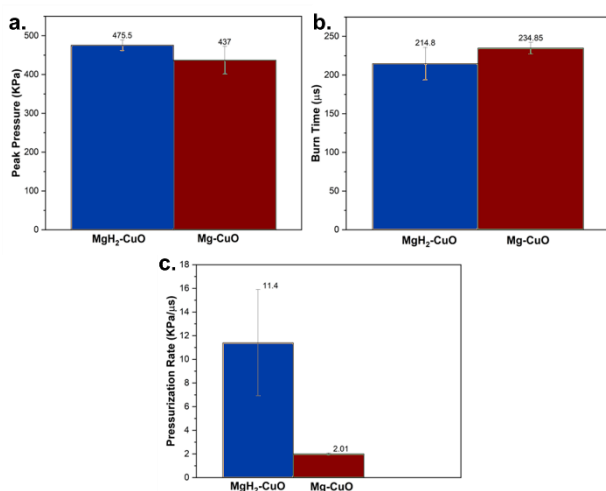


Figure 5. Pressure-cell test results comparing the (a) peak pressure, (b) burn time, and (c) pressurization rate of Mg and hydrogenated Mg NPs.

4. Conclusions

In conclusion, we developed a nonthermal plasma process for the surface functionalization of Mg NPs and investigated the effects on ignition. Our setup allows the gas-phase coating of Mg continuously under anaerobic conditions to prevent the formation of an oxide layer and circumvent diffusion-related barriers of atoms. Coating Mg with a Si-based shell results in lower ignition thresholds and faster combustion kinetics due to the close proximity of silicon oxides for faster diffusion of atoms. Additionally, in-flight surface modification of Mg NPs with hydrogen in oxygen-free conditions is achieved. Incorporating hydrogen with Mg particles increases the pressurization rate during combustion. This work shows that nonthermal plasma processing can realize new materials tailored for specific chemistries.

5. References

- [1] R. A. Yetter, G. A. Risha, S. F. Son, *Proceedings of the Combustion Institute*, **32**, 1819 (2009)
- [2] D. Sundaram, V. Yang, R. A. Yetter, *Progress in Energy and Combustion Science*, **61**, 293 (2017)
- [3] P. Ghildiyal, P. Biswas, S. Herrera, F. Xu, Z. Alibay, Y. Wang, H. Wang, R. Abbaschian, M. R. Zachariah, *ACS Applied Materials & Interfaces*, **14**, 17164 (2022)

- [4] D. L. Hastings, M. Schoenitz, K. M. Ryan, E. L. Dreizin, J. W. Krumpfer, *Propellants, Explosives, Pyrotechnics*, **45**, 621 (2020)
- [5] T. Hawa, M. R. Zachariah, *Journal of Aerosol Science*, **38**, 793 (2007)
- [6] G. Young, H. Wang, M. R. Zachariah, *Propellants Explos. Pyrotech.*, **40**, 413-418 (2015)
- [7] F. Xu, G. Nava, P. Biswas, I. Dulalia, H. Wang, Z. Alibay, M. Gale, D. J. Kline, B. Wagner, L. Mangolini, M. R. Zachariah, *Chemical Engineering Journal*, **430**, 133140 (2022)
- [8] K. F. Aguey-Zinsou, T. Nicolaisen, J. R. Ares Fernandez, T. Klassen, R. Bormann, *Journal of Alloys and Compounds*, **434-435**, 738-742 (2007)